

Existence of a phonon bottleneck for excitons in quantum dots

R. Heitz, H. Born, F. Guffarth, O. Stier, A. Schliwa, A. Hoffmann, and D. Bimberg

Institut für Festkörperphysik, Technische Universität Berlin, Sekr. PN 5-2, Hardenbergstraße 36, D-10623 Berlin, Germany

(Received 19 September 2001; published 29 November 2001)

A phonon bottleneck is manifested for correlated electron/hole (exciton) states in self-organized $\text{In}_x\text{Ga}_{1-x}\text{As}/\text{GaAs}$ quantum dots (QD's) with a flat, truncated shape. Suppressed relaxation and hot luminescence from excited states in the low-density regime are demonstrated. The long low-temperature relaxation time of ~ 7.7 ns, being ~ 15 times the radiative lifetime, is attributed to a quenched polar exciton-LO-phonon coupling in truncated QD's based on eight-band $\mathbf{k}\cdot\mathbf{p}$ model calculations.

DOI: 10.1103/PhysRevB.64.241305

PACS number(s): 78.67.Hc, 63.20.Ls, 73.21.La, 78.47.+p

Energy relaxation processes in semiconductor quantum dots (QD's) are a long standing problem interfering with the basic understanding of the phonon interaction in localized systems. QD's combine a weak phonon-coupling with a high oscillator strength due to the mesoscopic character of the wave functions.¹ Based on the weak coupling assumption, Fermi's Golden rule was used to estimate carrier relaxation rates in first and second order,²⁻⁴ predicting energy conservation to restrict relaxation in the subnanosecond region, i.e., faster than radiative recombination, to a narrow energy window around the LO-phonon energy (or multiples thereof). Thus relaxation between the discrete eigenstates of QD's will in general be slower than recombination processes due to the lack of suitable final states, leading to so-called "phonon bottleneck" effects.³

Time-resolved experiments point, however, to fast intradot relaxation in obvious contradiction to the expected phonon-bottleneck.⁵⁻⁷ The temperature dependence of the PL rise time⁵ and the near-resonant excitation behavior^{6,8-10} nevertheless support energy relaxation by inelastic LO-phonon scattering, suggesting predictions based on Fermi's Golden rule to fail for small QD's. Indeed, the nondiagonal elements of the Fröhlich coupling to LO phonons lead to the formation of vibronic (polaron) states,^{11,12} which might provide wide energy windows for efficient relaxation. The decay of such polaron states by the anharmonic decay of the involved phonon allows for fast relaxation on a few-ps time scale,^{13,14} being much shorter than typical radiative lifetimes.

Self-organized QD's provide an efficient means to test the influence of the polar exciton-LO-phonon coupling on the relaxation dynamics. The coupling strength, being proportional to the local charge density,¹ depends on the difference of the electron and hole wave functions^{15,16} and, thus, on the particular structural properties of such QD's. For instance, enhanced coupling is observed for pyramidal QD's.¹⁷

In this Rapid Communication, we report on the exciton dynamics in flat, truncated self-organized $\text{In}_x\text{Ga}_{1-x}\text{As}/\text{GaAs}$ QD's demonstrating the existence of a pronounced phonon bottleneck for excited electron/hole (exciton) states in photoluminescence (PL), PL excitation (PLE), and time-resolved PL (TRPL) experiments. Eight-band $\mathbf{k}\cdot\mathbf{p}$ model calculations show that the slow relaxation (~ 7.7 ns) of the resonantly excited exciton states is related to a quenched polar exciton-LO-phonon coupling in the flat QD's. A comparison to re-

sults for pyramidal QD's,^{18,19} suggests polaron formation to become important in case of enhanced coupling.¹⁷

The investigated $\text{In}_x\text{Ga}_{1-x}\text{As}/\text{GaAs}$ QD structures were grown by metal-organic chemical-vapor deposition on GaAs(001) substrate as described in Refs. 20 and 21. $\text{In}_x\text{Ga}_{1-x}\text{As}$ was deposited on top of small, capped InAs seed islands to increase the area density of the optically active $\text{In}_x\text{Ga}_{1-x}\text{As}$ QD's. Transmission electron microscopy images²¹ suggest a flat truncated pyramidlike shape for the $\text{In}_x\text{Ga}_{1-x}\text{As}/\text{GaAs}$ QD's with an average base length of ~ 20 nm and height of ~ 3 nm. The lateral QD density is $\sim 3 \times 10^{10} \text{ cm}^{-2}$.

Typical PL properties of the investigated $\text{In}_x\text{Ga}_{1-x}\text{As}/\text{GaAs}$ QD structures are shown in Fig. 1. Normalized PL spectra excited nonresonantly by an Ar^+ laser at various densities [panel (a)] show the ground state transition labeled I0 at 0.999 eV with a half-width of 34 meV and, at

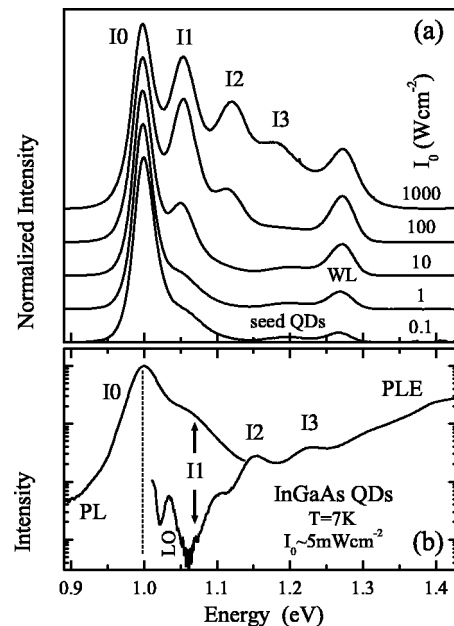


FIG. 1. PL and PLE spectra of $\text{In}_x\text{Ga}_{1-x}\text{As}/\text{GaAs}$ QD's. Panel (a) depicts PL spectra for various excitation densities ($E_{ex} = 2.41$ eV). The weak PL peaks at 1.19 eV and 1.27 eV are attributed to unpaired seed QD's and localized wetting layer states, respectively. Panel (b) compares the low-density PL to the PLE spectrum of the PL maximum.

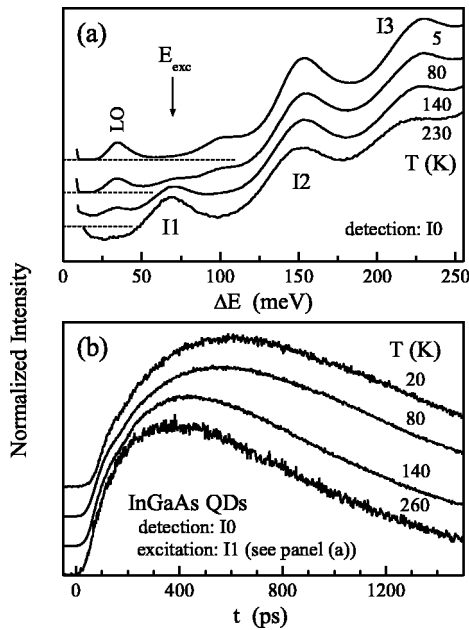


FIG. 2. (a) PLE spectra of the ground state PL and (b) corresponding transients for resonant excitation of I1 for various temperatures.

high excitation densities, three excited state transition groups labeled I1–3 with energy spacings between 65 meV and 80 meV.²² The expected substructure of these peaks^{15,16} is masked by inhomogeneous broadening and, thus, neglected describing the experimental results. Of particular interest is the unusual behavior of the first excited state transition I1. I1 maintains $\sim 16\%$ of the intensity of I0 even for excitation rates well below one exciton per QD and lifetime, suggesting hot luminescence. Indeed, the PLE spectrum of the ground state transition [panel (b)], which has been excited by a tungsten lamp dispersed by an 0.27-m double grating monochromator, shows LO-phonon-assisted ground state absorption¹⁷ at 1.034 eV but a minimum of the excitation efficiency in the spectral region of the I1 absorption. The results indicate unambiguously, that for the I1 state radiative recombination is more efficient than relaxation, causing recombination from a non-equilibrium exciton distribution.

The relaxation-limited dynamics is directly evident from TRPL measurements under resonant excitation of I1 [Fig. 2(b)] by ~ 1.5 ps long pulses of an optical parametric oscillator pumped by a ps-Ti:Sapphire laser. The PL was spectrally dispersed by a subtractive 0.35-m double grating monochromator and detected by a multi-channel-plate photomultiplier with an S1-cathode in time-correlated single-photon counting mode, providing for a system response to the laser pulses with a half-width of ~ 20 ps. At 20 K the intensity of the ground state transition I0 shows a slow rise and peaks with a delay of ~ 600 ps to the excitation. A least squares fit of two exponentials (convoluted with the system response) to the transient yields (480 ± 50) ps for both the rise (τ_{rise}) and decay (τ_{decay}) processes. Note that the rise time corresponds to the decay time observed for the resonant PL of I1 (not shown, equivalent results for similar samples have been reported recently).²³ Obviously, the relaxation of

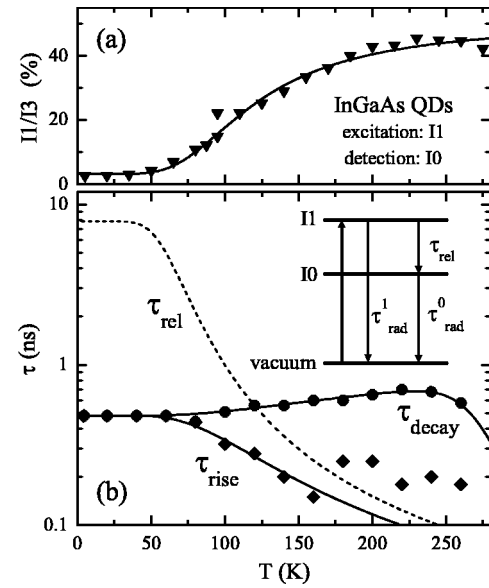


FIG. 3. Temperature dependency of the relaxation yield between I1 and I0 (a) and the lifetimes (b). Full lines represent a fit of the relaxation yield and the I1 lifetime within a three-level exciton scheme, which is depicted in the inset. The dashed line represents the extracted exciton relaxation time. The increase of the effective exciton lifetime with increasing temperature results from the thermal population of excited hole states having a lower recombination probability with the ground state electron.²⁴ Above ~ 220 K thermal escape of carriers becomes important.

the excited I1 state is the bottleneck in the excitation of the ground state I0, i.e., the rise time is determined by the balance of relaxation and recombination of the I1 state. The observation of multi-LO-phonon resonances in the PLE efficiency for InAs/GaAs QDs reported recently^{6,8–10} indicates direct relaxation of I1 to I0 in a single-step process, demonstrating that a simplified quasi-particle (exciton) term scheme as shown in Fig. 3(b) provides an adequate description of the dynamics.

Further insights into the relaxation process between I1 and I0 are obtained from temperature-dependent measurements. Figure 2(a) depicts PLE spectra of the ground state luminescence I0 for various temperatures. The spectra are normalized at the I3 resonance to compensate for thermal escape of carriers above ~ 220 K, which reduces also the ground state lifetime [Fig. 3(b)].²⁴ Above ~ 65 K excitation via the I1 absorption becomes gradually more efficient, indicating thermally activated relaxation. The temperature evolution of the intensity ratio I1/I3, being proportional to the relaxation yield between I1 and I0, is summarized in Fig. 3(a). The altered exciton dynamics reflects in the transients of the ground state PL I0 exciting resonantly the I1 exciton state 70 meV above the temperature-dependent ground state energy [Fig. 2(b)]. The rise of the ground state emission accelerates for temperatures above ~ 80 K. The derived rise and decay times are summarized in Fig. 3(b).

As outlined above, exciting resonantly the I1 state the dynamics can be described in a three-level exciton scheme [inset of Fig. 3(b)] composed of the vacuum level, I0, and I1, which accounts for radiative recombination of I0 (τ_{rad}^0) and

I1 (τ_{rad}^1) and relaxation from I1 to I0 (τ_{rel}). Thereby, a temperature-dependent relaxation rate $1/\tau_{rel} = 1/\tau_{rel}^0 [B + n_B(E_a, T)]$ was assumed, with n_B the Bose distribution, E_a the activation energy, and B a temperature-independent contribution (e.g., spontaneous relaxation at low temperatures).

Solid lines in Fig. 3 represent a fit of the relaxation yield $\eta = \tau_{rad}^1 / (\tau_{rad}^1 + \tau_{rel})$ (\sim I1/I3) [panel (a)] and the lifetime of I1 $\tau_{rise} = \tau_{rad}^1 \tau_{rel} / (\tau_{rad}^1 + \tau_{rel})$ [panel (b)]. The best fit yields a radiative lifetime τ_{rad}^1 of 520 ps for I1, being only slightly larger than that of I0 ($\tau_{rad}^0 = 480$ ps). The activation energy E_a of the relaxation process is with (33 ± 4) meV in good agreement with typical LO-phonon energies of InAs/GaAs QD's,^{17,18} supporting inelastic LO-phonon scattering to dominate the relaxation rate. The derived temperature-independent relaxation contribution $B = 0.0039 \pm 0.0002$ is, however, much lower than unity, which would be expected for a resonant one-LO-phonon process. The small spontaneous relaxation rate is attributed to the higher-order character of the relaxation process: For the given relaxation energy of ~ 70 meV, two LO phonons as well as the coupling to acoustic phonons are required to maintain energy conservation. The dashed line in Fig. 3(b) represents the extracted thermally activated relaxation time (τ_{rel}). The relaxation time is as long as ~ 7.7 ns, being ~ 15 times the radiative lifetime (τ_{rad}^1), below 60 K and decreases to ~ 80 ps at 300 K. At 120 K the radiative lifetime and the relaxation time are equal marking the transition from relaxation- to recombination-limited exciton dynamics.

The present results are in contrast to previous ones for pyramidal InAs QD's, for which even at He temperatures recombination-limited exciton dynamics was observed exciting resonantly I1, i.e., $\tau_{rel}^1 \ll \tau_{rad}^1$.^{18,19} We propose the different exciton dynamics to result from the shape-dependent electron/hole overlap, thus, reflecting the different structural properties of the respectively investigated QD's.

In pyramidal QD's the symmetry-lowering to C_{2v} by the atomic structure anisotropy and the piezoelectric effect leads to different elongation directions for electron and hole wave functions.^{15,16,25} The effects are caused by the inequivalent side facets and edges, respectively. Truncating such QD's gradually restores the C_{4v} symmetry of the electron and hole wave functions as is shown in Fig. 4, depicting exciton properties for InAs/GaAs QD's of systematically varying shape predicted by eight-band $\mathbf{k} \cdot \mathbf{p}$ calculations in the Hartree approximation.^{16,19,25} A pyramidal QD with a base length of 17 nm was successively truncated redistributing the InAs to maintain a constant volume. Panel (a) shows the effect of the side facets and edges to decrease with decreasing aspect ratio: The fine structure splitting of the first excited state transition I1 at ~ 1.1 eV decreases and the electron and hole wave functions become more similar (see the insets for the exciton ground state in the two limiting cases). Panel (b) shows the Huang-Rhys factor calculated for the Fröhlich coupling to LO phonons, which is a measure for the coupling strength of a particular exciton state.^{1,17,25} Truncating pyramidal QD's decreases the coupling for "allowed" transitions with a large oscillator strength and, simultaneously, increases

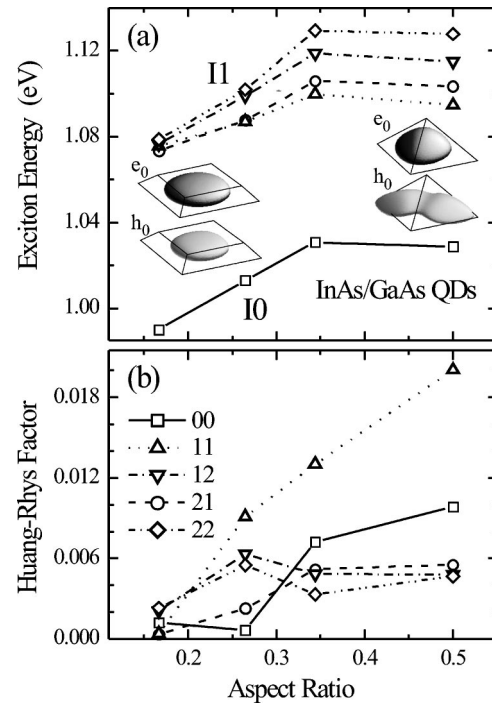


FIG. 4. Calculated transition energy (a) and Huang-Rhys factor (b) of exciton states in truncated pyramidal InAs/GaAs QD's as a function of the aspect ratio. The insets of panel (a) display electron and hole wave functions of the ground state exciton in full pyramidal (right) and the flattest truncated (left) QD's, respectively. The calculations are described in the text.

the oscillator strength of the ground state transition I0 by about two times (not shown). The calculations will be presented in detail elsewhere.²⁶

The shape-dependent electron and hole wave functions provide for a qualitative understanding of the different exciton dynamics in pyramidal and truncated QD's. On the one hand, the increased electron-hole overlap accounts for a shorter ground state lifetime in truncated QD's (~ 480 ps) compared to that in pyramidal ones (~ 975 ps).¹⁸ On the other hand, the concomitant variation of the polar exciton-LO-phonon coupling [panel (b)] explains the suppressed exciton relaxation in truncated QD's as well as faster relaxation in pyramidal QD's. The average Huang-Rhys factor of the four exciton states constituting the I1 peak, weighted by the respective oscillator strength, decreases by more than one order of magnitude when truncating the QD's.

The temperature and shape dependencies of the relaxation dynamics confirm phonon-assisted relaxation for the strongly localized exciton states in self-organized QD's and put an upper limit on the probabilities of competing channels like Auger-type²⁷ or Coulomb-scattering processes. Note, that the phonon bottleneck is observed for the optically active I1 exciton state. PLE spectra [e.g., Fig. 1(b)] show efficient population of the ground state I0 exciting the GaAs barrier, the WL, as well as the excited exciton states I2 and I3. Obviously, excitons excited in higher energy states have additional, more efficient relaxation channels, which do not involve I1 as an intermediate state. For nonresonant excitation only $\sim 16\%$ of the excitons end up in the I1 state, Fig. 1(a).

Both, Auger-type processes²⁷ and a stronger polar LO-phonon coupling of the involved exciton states²⁶ might contribute to fast relaxation of the higher excited states as indeed observed in corresponding TRPL experiments.^{5,6,23}

In conclusion, suppressed exciton relaxation has been demonstrated for self-organized $\text{In}_x\text{Ga}_{1-x}\text{As}/\text{GaAs}$ QD's. A low-temperature relaxation time of ~ 7.7 ns leads to a pronounced phonon-bottleneck effect and hot luminescence from the first excited exciton state. The temperature dependencies of the relaxation time and yield support inelastic phonon-scattering as dominant relaxation mechanism. The relaxation-limited exciton dynamics is attributed to the quenched polar exciton-LO-phonon coupling and large radiative recombination probability in the investigated, truncated

QD's based on eight-band $\mathbf{k}\cdot\mathbf{p}$ model calculations. The results suggest that depending on the QD shape, i.e., the polar exciton-LO-phonon coupling strength, either the formation of excitonic polarons, providing for recombination-limited dynamics, or Fermi's Golden rule, explaining relaxation-limited dynamics with a phonon-bottleneck, are applicable.

Parts of this work were supported by the Deutsche Forschungsgemeinschaft in the framework of Sonderforschungsbereich 296. Parts of the electronic structure calculations were performed on the Cray T3E computer of the Konrad-Zuse-Zentrum für Informationstechnik Berlin within project Bvpt13.

- ¹S. Schmitt-Rink, D.A.B. Miller, and D.S. Chemla, *Phys. Rev. B* **35**, 8113 (1987).
- ²B. Bockelmann and G. Bastard, *Phys. Rev. B* **42**, 8947 (1990).
- ³H. Benisty, C.M. Sotomayor-Torres, and C. Weisbuch, *Phys. Rev. B* **44**, 10 945 (1991).
- ⁴T. Inoshita and H. Sakaki, *Phys. Rev. B* **46**, 7260 (1992).
- ⁵B. Ohnesorge, M. Albrecht, J. Oshinowo, A. Forchel, and Y. Arakawa, *Phys. Rev. B* **54**, 11 532 (1996).
- ⁶R. Heitz, M. Veit, N.N. Ledentsov, A. Hoffmann, D. Bimberg, V.M. Ustinov, P.S. Kop'ev, and Zh.I. Alferov, *Phys. Rev. B* **56**, 10 435 (1997).
- ⁷T.S. Sosnowskii, T. Norris, H. Jiang, J. Singh, K. Kamat, and P. Bhattacharya, *Phys. Rev. B* **57**, 9423 (1998).
- ⁸R. Heitz, M. Grundmann, N.N. Ledentsov, L. Eckey, M. Veit, D. Bimberg, V.M. Ustinov, A.Yu. Egorov, A.E. Zhukov, P.S. Kop'ev, and Zh.I. Alferov, *Appl. Phys. Lett.* **68**, 361 (1996).
- ⁹M.J. Steer, D.J. Mowbray, W.R. Tribe, M.S. Skolnick, M.D. Sturge, M. Hopkinson, A.G. Cullis, C.R. Whitehouse, and R. Murray, *Phys. Rev. B* **54**, 17 738 (1996).
- ¹⁰K.H. Schmidt, G. Medeiros-Ribeiro, M. Oestereich, P.M. Petroff, and G.H. Döhler, *Phys. Rev. B* **54**, 11 346 (1996).
- ¹¹S. Hameau, Y. Guldner, O. Verzelen, R. Ferreira, G. Bastard, J. Zeman, A. Lemaitre, and J.M. Gérard, *Phys. Rev. Lett.* **83**, 4152 (1999).
- ¹²T. Stauber, R. Zimmermann, and H. Castella, *Phys. Rev. B* **62**, 7336 (2000).
- ¹³X.-Q. Li, H. Nakayama, and Y. Arakawa, *Phys. Rev. B* **59**, 5069 (1999).
- ¹⁴O. Verzelen, R. Ferreira, and G. Bastard, *Phys. Rev. B* **62**, R4809 (2000).
- ¹⁵L.-W. Wang, J. Kim, and A. Zunger, *Phys. Rev. B* **59**, 5678 (1999).
- ¹⁶O. Stier, M. Grundmann, and D. Bimberg, *Phys. Rev. B* **59**, 5688 (1999).
- ¹⁷R. Heitz, I. Mukhametzanov, O. Stier, A. Madhukar, and D. Bimberg, *Phys. Rev. Lett.* **83**, 4654 (1999).
- ¹⁸R. Heitz, H. Born, I. Mukhametzanov, A. Hoffmann, A. Madhukar, and D. Bimberg, *Appl. Phys. Lett.* **77**, 3746 (2000).
- ¹⁹R. Heitz, O. Stier, I. Mukhametzanov, A. Madhukar, and D. Bimberg, *Phys. Rev. B* **62**, 11 017 (2000).
- ²⁰F. Heinrichsdorff, M. Grundmann, O. Stier, A. Krost, and D. Bimberg, *J. Cryst. Growth* **195**, 540 (1998).
- ²¹R. Sellin, N.N. Ledentsov, D. Bimberg, V.M. Ustinov, and Zh.I. Alferov, in *Proceedings of the 6th International Symposium in Advanced Physics of Fields*, edited by N. Koguchi (National Research Institute for Metals, Tsukuba, 2001), p. 49.
- ²²The transition energies are renormalized by many-particle interactions in the presence of spectator excitons (R. Heitz, F. Guffarth, M. Grundmann, A. Madhukar, and D. Bimberg, *Phys. Rev. B* **62**, 16 881 (2000)).
- ²³R. Heitz, H. Born, T. Lüttgert, A. Hoffmann, and D. Bimberg, *Phys. Status Solidi B* **221**, 65 (2000).
- ²⁴R. Heitz, I. Mukhametzanov, A. Madhukar, A. Hoffmann, and D. Bimberg, *J. Electron. Mater.* **28**, 520 (1999).
- ²⁵O. Stier, *Electronic and Optical Properties of Quantum Dots and Wires*, Vol. 7 of *Berlin Studies in Solid State Physics* (Wissenschaft und Technik Verlag, Berlin, 2001).
- ²⁶O. Stier, A. Schliwa, R. Heitz, and D. Bimberg (unpublished).
- ²⁷R. Ferreira and G. Bastard, *Appl. Phys. Lett.* **74**, 2818 (1999).